Biomacromolecules

ARTICLE

pubs.acs.org/Biomac

Biocatalytic Route to Sugar-PEG-Based Polymers for Drug Delivery Applications

Sumati Bhatia,[†] Andreas Mohr,[‡] Divya Mathur,[†] Virinder S. Parmar,[†] Rainer Haag,[*,‡] and Ashok K. Prasad[*,†]

[†]Bioorganic Laboratory, Department of Chemistry, University of Delhi, Delhi-110 007, India

[‡]Institute for Chemistry and Biochemistry, Free University Berlin, Takustr. 3, D- 14195 Berlin, Germany

Supporting Information

ABSTRACT: Sugar-PEG-based polymers were synthesized by enzymatic copolymerization of 4-*C*-hydroxymethyl-1,2-*O*-isopropylidene-*β*-L-*threo*-pentofuranose/4-*C*-hydroxymethyl-1,2-*O*-benzylidene-*β*-L-*threo*-pentofuranose/4-*C*-hydroxymethyl-1,2-*O*-isopropylidene-3-*O*-pentyl-*β*-L-*threo*-pentofuranose with PEG-600 dimethyl ester using Novozyme-435 (*Candida antarctica* lipase immobilized on polyacrylate). Carbohydrate monomers were obtained by the multistep synthesis starting from diacetone-D-glucose and PEG-600 dimethyl ester, which was in turn obtained by the esterification of the commercially available PEG-600 diacid. Aggregation studies on the copolymers revealed that in aqueous solution those polymers bearing the hydrophobic pentyl/benzylidene moiety spontaneously self-assembled into supramolecular aggregates. The critical aggregation concentration (CAC) of polymers was determined by surface tension measurements, and the precise size of the aggregates was obtained by dynamic light scattering. The polymeric aggregates were further explored for their drug encapsulation properties in buffered aqueous solution of pH 7.4 (37 °C) using nile red as a hydrophobic model compound by means of UV/vis and fluorescence spectroscopy. There was no significant encapsulation in polymer synthesized from 4-*C*-hydroxymethyl-1,2-*O*-isopropylidene-*β*-L-*threo*-pentofuranose because this sugar monomer does not contain a big hydrophobic moiety as the pentyl or the benzylidene moiety. Nile red release study was performed at pH 5.0 and 7.4 using fluorescence spectroscopy. The release of nile red from the polymer bearing benzylidene moiety and pentyl moiety was observed with a half life of 3.4 and 2.0 h, respectively at pH 5.0, whereas no release was found at pH 7.4.

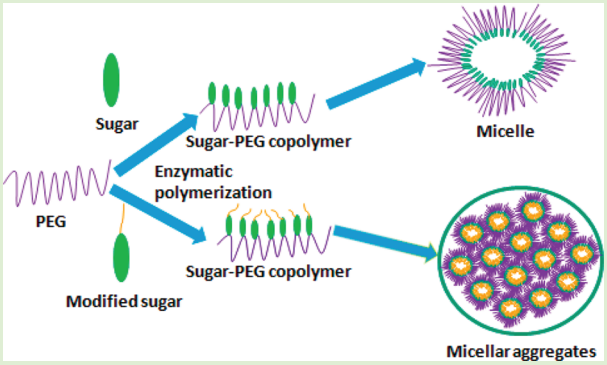

INTRODUCTION

There is always a need to have biocompatible drug carriers capable of delivering water insoluble drugs with high transport and controlled release capacity. Poly(ethylene glycol) (PEG) and the materials derived from it are highly applicable in biotechnology and pharmacology. This is due to the excellent water solubility and high biocompatibility of PEG. PEGylation has proved to be a successful approach to drug delivery.[1] Carbohydrates are known for their target specificity and also as promising candidates for homing molecules.[2,3] Moreover, the effectiveness of a drug carrier is determined by its ability to control the time over which drug release occurs or to trigger the drug release at a specific location. Drug release can be controlled by stimuli or a host-responsive process. In recent years, drug carriers that were responsive to their environment or to external stimuli have been designed. For example, temperature has been used to modulate drug release from thermoresponsive micelles,[4] ultrasound has been reported to trigger drug release from pluronic micelles,[5] and change in pH has also been exploited as a useful stimulus in the development of a drug carrier. Numerous pH gradients exist in both normal and pathophysiological states, and it is well-established now that extracellular pH of solid tumors is significantly more acidic than normal tissues, with a mean pH of 6.5 in comparison to 7.4 for the blood and normal tissues.[6−9] Therefore, polymeric micelles that are responsive to pH gradients can be designed to release their payload selectively in tumor tissue or within tumor cells.[10−12]

Several approaches can be taken to design pH-sensitive drug carriers.[13] One approach is to directly attach the drug to the drug carrier by acid degradable linkages. For example, this approach was used by Park et al.[14] where doxorubicin was chemically conjugated to the terminal end of poly(L-lactic acid) in diblock copolymer of PLLA-PEG by acid cleavable hydrazone and *cis*-aconityl bond. Another approach is the incorporation of acid-cleavable hydrophobic groups into the copolymer. Such hydrophobic groups interact with water insoluble hydrophobic drug molecule and hold it by noncovalent forces until they reach certain acidic condition. Hydrophobic groups that are drug

Received: May 12, 2011
Revised: July 29, 2011
Published: August 12, 2011

Scheme 1. Synthesis of the Monomers 2, 5, and 8

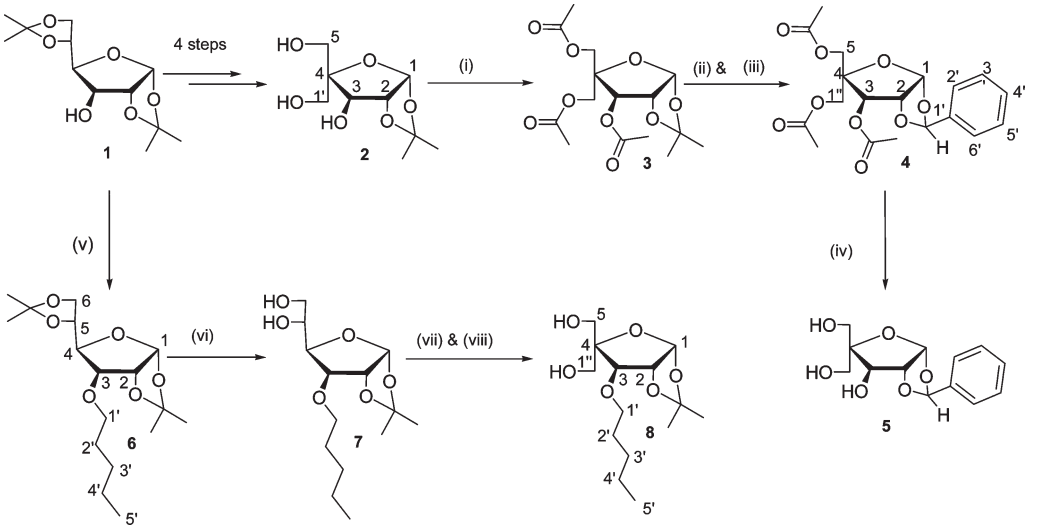

[a] Reagents and conditions: (i) Ac_2O, DMAP, THF, 90%; (ii) 70% AcOH−H_2O, 50 °C; (iii) $PhCH(OMe)_2$, CSA, DMF, 40%; (iv) K_2CO_3, dry MeOH, 88%; (v) $C_5H_{11}Br$, TBAI, NaOH, dry DMF, 87%; (vi) 60% AcOH-H_2O, 82%; (vii) $NaIO_4$, CH_2OHCH_2OH, THF:H_2O; and (viii) HCHO, 2 M NaOH, dioxane:H_2O, 69%.

holding groups in the copolymeric drug carrier are hydrolyzed under acidic conditions, and the drug carrier releases its payload. In the recent past, several pH-responsive block copolymeric systems have been designed, synthesized, and studied for their self-assembling properties and release of hydrophobic drugs.[10,13−15] For example, Kataoka et al.[16] have synthesized and used poly(ethylene glycol)-poly(L-lysine) block copolymer as a pH-sensitive drug delivery agent for the delivery of photosensitizer drugs for cancer therapy. Chen et al.[17] has reported the synthesis of pH-responsive biodegradable micelles bearing acid sensitive trimethoxybenzylidene acetal and exploited it for the encapsulation and release study of paclitaxel and doxorubicin. Furthermore, pH-sensitive polymersomes have also been synthesized for the encapsulation and release study of drugs like paclitaxel and doxorubicin.[18]

So far, sugar-PEG polymeric systems have not been explored much for pH-responsive drug delivery applications. In the present article, we report the biocatalytic synthesis of novel sugar-PEG-based copolymeric architectures bearing acid cleavable groups. These biocatalytically synthesized sugar-PEG-based polymeric architectures have been studied for their molecular aggregation, drug encapsulation, and drug release behavior using nile red as a model drug.

EXPERIMENTAL SECTION

Materials. Reactions requiring dry conditions were carried out under argon. Analytical TLCs were performed on precoated Merck silica-gel $60F_{254}$ plates; silica gel (100−200 mesh) was used for column chromatography. Dry and analytical-grade solvents and reagents were purchased from Sigma-Aldrich and Acros chemical companies. Novozyme-435 was a gift from Novozymes A/s (Copenhagen, Denmark). Nile red was obtained from ABCR (76187 Karlsruhe, Germany). Water of Millipore quality (resistivity ~18 MΩ·cm^{-1}, pH 5.6 ± 0.2) was used in all experiments and for preparation of all samples. Buffers of 0.01 and 0.10 M phosphate were prepared by weight from $Na_2HPO_4 \cdot 7H_2O$ and $NaH_2PO_4 \cdot H_2O$. For acidic pH (5.0), acetate buffer of 0.1 M was employed. pH values were measured with a Piccolo Plus ATC pH/C meter at 25 °C.

Instrumentation. *Nuclear Magnetic Resonance Spectroscopy.* The ^1H and ^{13}C and DEPT NMR spectra were recorded on a Bruker DRX 400 spectrometer operating at 400 and 100 MHz, respectively. Bruker AMX 500 MHz spectrometer was used to record 2D NMR spectrum ($^1H-^1H$ correlation spectrum and $^1H-^{13}C$ correlation spectrum). The spectra were calibrated on the solvent peak ($CDCl_3$: δ 7.26 for ^1H NMR and δ 77.0 for ^{13}C NMR; CD_3OD: δ 4.84 for ^1H NMR and δ 49.05 for ^{13}C NMR).

Infrared Spectroscopy, ESI, and Melting Point Measurements. Infrared (IR) spectra were recorded as thin films between KBr or CaF_2 plates on a Bruker IFS 66 FT-IR spectrometer. For ESI measurements a TSQ 7000 (Finnigan Mat) instrument and for high-resolution mass spectra a JEOL JMS-SX-102A spectrometer was used. Melting points of solid compounds were taken on a BUCHI melting point apparatus M-560.

Gel Permeation Chromatography. Molecular weight and molecular weight distribution $\overline{M}_w/\overline{M}_n$ of polymers were determined using gel permeation chromatography (GPC) equipped with an agilent 1100 pump, refractive index detector, and PLgel and Suprema columns. The eluent was THF or water with a flow rate of 1.0 mL/min. The molecular weights were calibrated with polystyrol or pullulan standards.

Surface Tension Measurements. Critical aggregation concentration (CAC) of the polymers was determined by a commercially available pendant drop tensiometer OCA 20 built by Dataphysics, Germany. Aqueous sample concentrations in Milli-Q water were prepared 24 h before measurement. Calculation of the surface tension was done by using the Young−Laplace Equation. In a typical experiment, the aggregation behavior of the polymers in water was studied over the concentration range of 7×10^{-7} to 1×10^{-3} M. The surface tension of each hanging drop was determined two times per minute, and the measurement was stopped when the surface tension did not change by more than 0.1 mN/m over 2 min. Equilibration time was generally between 25 and 70 min at lower concentrations. All measurements were done at 25.0 ± 0.5 °C.

Light Scattering Measurements. Dynamic light scattering measurements were performed to determine the precise size of the micelle/polymeric aggregates in aqueous solution. Measurements were carried

out on a Zetasizer Nano ZS analyzer with integrated 4 mW He−Ne laser, λ = 633 nm (Malvern Instruments, Worcestershire WR14 1XZ, U.K.). This instrument, which uses the backscattering detection (scattering angle θ = 173°) and an avalanche photodiode detector, is equipped with a helium−neon laser source (operating wavelength 633 nm; power 4.0 mW) and a thermostatted sample chamber controlled by a thermoelectric peltier. For the measurement of size, aqueous solution of copolymer **11** at the concentration of 5 g/L and copolymers **12** and **13** at the concentration of 1 g/L were prepared in Milli-Q water and vigorously stirred for 12 h at room temperature (37 °C). Solutions were filtered via 0.45 μm polytetrafluoroethylene (PTFE) filters and then allowed to equilibrate for 6 h at room temperature (37 °C). These copolymeric aqueous solutions were used for dynamic light scattering measurements. For all experiments, disposable UV-transparent cuvettes (12.5 × 12.5 × 45 mm, Sarstedt AG, 51582 Nümbrecht, Germany) were used.

Transmission Electron Microscopy. TEM images of polymers were taken on CM12 TEM (compaTEM ny FEI) instrument operating at a high tension of 100 KV at a magnification of 60.000. 4.5% phosphotungstic acid (PTA) with 0.1% trehalose was used as staining material. A droplet of the aqueous sample solution (5 μL at the concentration of 5 g/L) was taken on the copper grid (covered with a 7 nm film of carbon) coated with collodion for 60 s. After blotting, a drop of staining material was added for 60 s. The grid was again blotted and dried at room temperature for at least 1 h before images were taken.

Absorbance and Fluorescence Measurements. Absorption spectra were recorded between 220 and 800 nm using a Scinco S-3150 UV/vis spectrophotometer (range: 187−1193 nm; resolution: 1024 points). All measurements were carried out in 10 mM phosphate buffer in a thermostatted UV-cell (1 cm). Fluorescence emission spectra were taken with a Jasco FP-6500 spectrofluorimeter equipped with a thermostatted cell holder, a DC-powered 150 W xenon lamp, a Hamamatsu R928 photomultiplier, and a variable slit system. Emission spectra were recorded from 575 to 800 nm after excitation at 550 nm. Both excitation and emission slits were set at 5 nm. For release studies, the intensity of the emission spectrum of nile red was monitored as a function of time at pH 5.0 and physiological pH (7.4) by maintaining the temperature at 37.0 ± 0.1 °C. Data were fitted to the relation $I_t = I_0 \cdot \exp(-k_{obs} \cdot t)$. Here I_t describes the intensity measured at time t, and I_0 denotes the initial fluorescence intensity. The half-life time is given by the simple relationship $t_{1/2} = \ln(2)/k_{obs}$.

RESULTS AND DISCUSSION

Synthesis of Carbohydrate Monomers 2, 5, and 8. The trihydroxy compound 4-*C*-hydroxymethyl-1,2-*O*-isopropylidene-β-L-*threo*-pentofuranose (**2**) was prepared starting from commercially available diacetone-D-glucose **1** by following the modified procedure of Youssefyeh et al.[19] and Christensen et al.[20] and unambiguously identified on the basis of its spectral data (^{1}H NMR, ^{13}C NMR, IR spectra, and HRMS) analysis and comparison of the spectral data with those reported in the literature[19] (Scheme 1). Furthermore, the trihydroxy sugar derivative **2** was peracetylated with acetic anhydride in the presence of catalytic amount of DMAP in THF to afford 4-*C*-acetoxymethyl-3,5-di-*O*-acetyl-1,2-*O*-isopropylidene-β-L-*threo*-pentofuranose **3** in 90% yield. Deprotection of 1,2-*O*-isopropylidene protection in compound **3** was achieved using an aqueous solution of AcOH (70%) at 50 °C, and the crude triacetoxy sugar derivative obtained was used as such for the 1,2-*O*-benzylidene protection using benzaldehyde dimethylacetal in the presence of camphor sulfonic acid (CSA)[21−23] as catalyst to afford 4-*C*-acetoxymethyl-3,5-di-*O*-acetyl-1,2-*O*-benzylidene-β-L-*threo*-pentofuranose (**4**) in 40% yield. The triacetylated sugar compound **4** was completely deacetylated using K_2CO_3 in dry methanol[24] to obtain the benzylidene sugar monomer, that is, 4-*C*-hydroxymethyl-1,2-*O*-benzylidene-β-L-*threo*-pentofuranose (**5**) in 88% yield (Scheme 1).

Scheme 2. Synthesis of PEG Dimethyl Ester

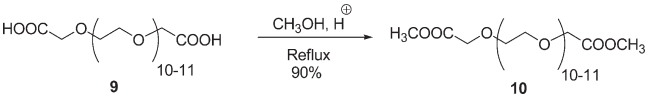

Furthermore, for the synthesis of C-3-*O*-pentyl pentofuranosyl sugar monomer **8**, diacetone-D-glucose **1** was treated with bromopentane in dry DMF in the presence of sodium hydroxide, phase transfer catalyst tetrabutyl ammonium iodide, and molecular sieves to afford, 1,2:5,6-di-*O*-isopropylidene-3-*O*-pentyl-β-L-*threo*-pentofuranose (**6**) in 87% yield. In this context, it is worthwhile to mention that the same alkylation reaction has been performed on other substrates in the presence of expensive base CsOH.[25] The more labile 5,6-*O*-isopropylidene acetal in *C*-3 pentyloxy sugar derivative **6** was selectively hydrolyzed by aqueous acetic acid to obtain 1,2-*O*-isopropylidene-3-*O*-pentyl-D-glucofuranose (**7**) in 82% yield. Oxidative cleavage of the two vicinal hydroxyl groups in compound **7** afforded the corresponding aldehyde, which was subjected to aldol-canizzaro reaction[19,26] to give the 4-*C*-hydroxymethyl-1,2-*O*-isopropylidene-3-*O*-pentyl-β-L-*threo*-pentofuranose (**8**) in 69% yield (Scheme 1).

Synthesis of the PEG Dimethyl Ester 10. The commercially available polyethylene glycol *bis*(carboxymethyl) ether ($\overline{M}_n$ 600) (**9**) was esterified into poly[ethylene glycol *bis*(carboxymethyl) ether] dimethyl ester (**10**) in a single-step reaction by refluxing the substrate in methanol in the presence of a catalytic amount of H_2SO_4 in almost quantitative yield (Scheme 2).

All synthesized compounds **2**−**8** and **10** were unambiguously identified on the basis of their spectral (IR, ^{1}H and ^{13}C NMR, DEPT-135 NMR spectra, and HRMS) data analysis. The structures of the known compounds **2** and **10** were further confirmed by comparing their physical and spectral data with those reported in the literature.[19,27]

Synthesis of Polymers 11−13. Lipases have been used for selective esterification/transesterification reactions in the enzyme-mediated organic synthesis.[28,29] Furthermore, one of the lipases, viz. Novozyme-435 (*Candida antarctica* lipase immobilized on polyacrylate), has been explored for carrying out selective reactions necessary for carbohydrate modifications[30−32] and polymer synthesis.[33−36] Taking lead from our previous experience of using lipases for discrimination between the two ester functions of triacylated pentofuranose derivatives with an aim to synthesize bicyclonucleosides,[25,30,31] Novozyme-435 lipase was used to affect the copolymerization reaction of hydroxy sugar monomers **2**, **5**, or **8** with the PEG dimethyl ester **10** under high vacuum and solventless conditions at 70 °C to synthesize poly-[polyoxyethylene-oxy-*bis*(carboxymethyl)-4-methylene-1,2-*O*-isopropylidene-β-L-*threo*-pentofuranosyl] (**11**), poly[polyoxyethylene-oxy-*bis*(carboxymethyl)-4-methylene-1,2-*O*-benzylidene-β-L-*threo*-pentofuranosyl] (**12**), and poly[polyoxyethylene-oxy-*bis*(carboxymethyl)-4-methylene-1,2-*O*-isopropylidene-3-*O*-pentyl-β-L-*threo*-pentofuranosyl] (**13**) in 72, 54, and 67% yields, respectively. All three polymerization reactions when performed under identical conditions but without adding lipase did not yield any product. To our knowledge, it is the first example of transesterification reaction involving tri/dihydroxy sugar derivatives

Scheme 3. Biocatalytic Route to the Sugar-PEG-Based Polymers 11−13

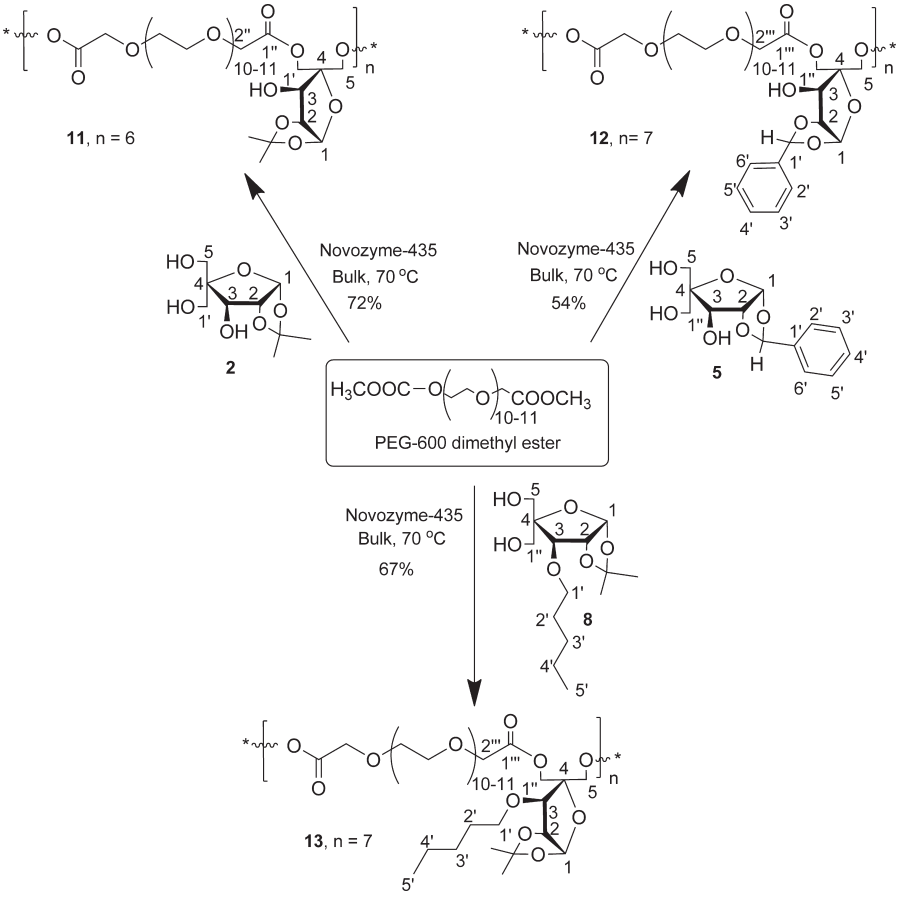

and PEG dimethyl ester leading to the formation of copolymers **11**−**13** (Scheme 3). All three polymers **11**−**13** were unambiguously characterized from their IR, ^{1}H NMR, ^{13}C NMR, DEPT-135 NMR, and 2D NMR spectral data analysis.

Characterization of Polymers 11−13. *Poly[polyoxyethylene-oxy-bis(carboxymethyl)-4-methylene-1,2-O-isopropylidene-β-L-threo-pentofuranosyl] (**11**).* In the ^{1}H NMR spectrum of polymer **11**, the C-5H and C-1′H recorded a downfield shift of 0.54 to 0.69 ppm and resonated at δ 4.11−4.39 (m) with respect to the same protons resonating at δ 3.57−3.70 (m) in the corresponding monomer 4-*C*-(hydroxymethyl)-1,2-*O*-isopropylidene-β-L-*threo*-pentofuranose (**2**). The downfield shift in the chemical shift value of C-5H and C-1′H in the polymer revealed that the two primary hydroxyl groups at the corresponding positions in the starting compound **2** were engaged in copolymerization over the lone secondary hydroxyl group present at C-3 position in the monomer **2**. Therefore, the lipase exhibited regioselectivity and recognized the two primary hydroxyl groups in the monomer **2** for transesterification reaction with PEG dimethyl ester **10**. This was further supported by the fact that there was no appreciable change in the chemical shift value of C-3H (δ 4.26) in the ^{1}H NMR spectrum of polymer **11** with respect to the chemical shift value of the same proton (δ 4.20) in the monomer **2**. The chemical shift value δ 4.26 of C-3H in the ^{1}H NMR spectrum of polymer **11** was confirmed by the ^{1}H−^{13}C correlation spectrum (Figure 1), whereas the chemical shift value of C-3 in the ^{13}C NMR spectrum of the polymer was confirmed by DEPT-135 NMR (Figure 2). The presence of all other −CH, $-CH_2$, and $-CH_3$ groups in the polymer **11** were confirmed by its DEPT-135 NMR spectrum. The number-average molecular weight of the polymer **11** as obtained by GPC in H_2O (1 mL/min.) was 4408 g/mol with polydispersity index (PDI) of 1.96, which indicates the presence of approximately six monomeric units in the polymer.

*Poly[polyoxyethylene-oxy-bis(carboxymethyl)-4-methylene-1,2-O-benzylidene-β-L-threo-pentofuranosyl] (**12**).* In the ^{1}H NMR spectrum of polymer **12**, the C-5H and C-1″H recorded a downfield shift of 0.47 to 0.56 ppm and resonated at δ 4.08−4.38 (m) with respect to the same protons resonating at δ 3.61−3.82 (m) in the corresponding monomer 4-*C*-(hydroxymethyl)-1,2-*O*-benzylidene-β-L-*threo*-pentofuranose (**5**). The downfield shift in the chemical shift value of C-5H and C-1″H in the polymer revealed that the two primary hydroxyl groups at the corresponding positions in the starting compound **5** were engaged in copolymerization over the lone secondary hydroxyl group present at C-3 position in the monomer **5**. Therefore, the lipase exhibited regioselectivity and recognized the two primary hydroxyl groups in the monomer **5** for transesterification reaction with PEG dimethyl ester **10**. This was further supported by the fact that there was no appreciable change in the chemical shift value of C-3H (δ 4.27) in the ^{1}H NMR spectrum of polymer **12** with respect to the chemical shift value of the same proton (δ 4.25) in the monomer **5**. The chemical shift value δ 4.27 of C-3H in the ^{1}H NMR spectrum of polymer **12** was confirmed by ^{1}H−^{13}C correlation spectrum (Figure 3), whereas the chemical shift value of C-3 in the ^{13}C NMR spectrum of the polymer was confirmed by DEPT-135 NMR (Figure 4).

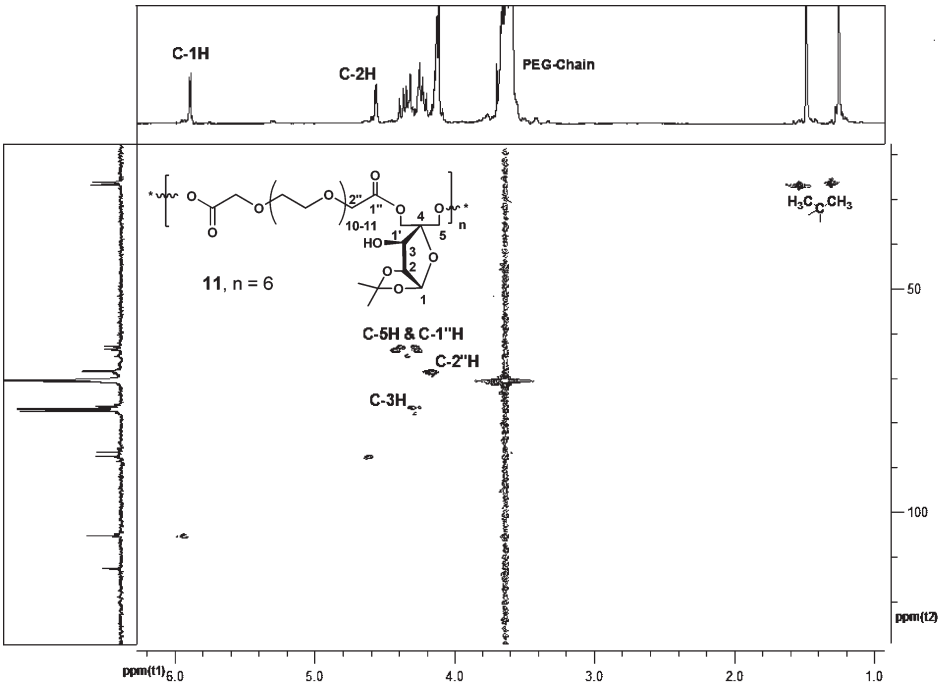

Figure 1. $^{1}H-^{13}C$ correlation spectrum (Bruker AMX-500, chloroform-*d*) of polymer **11**.

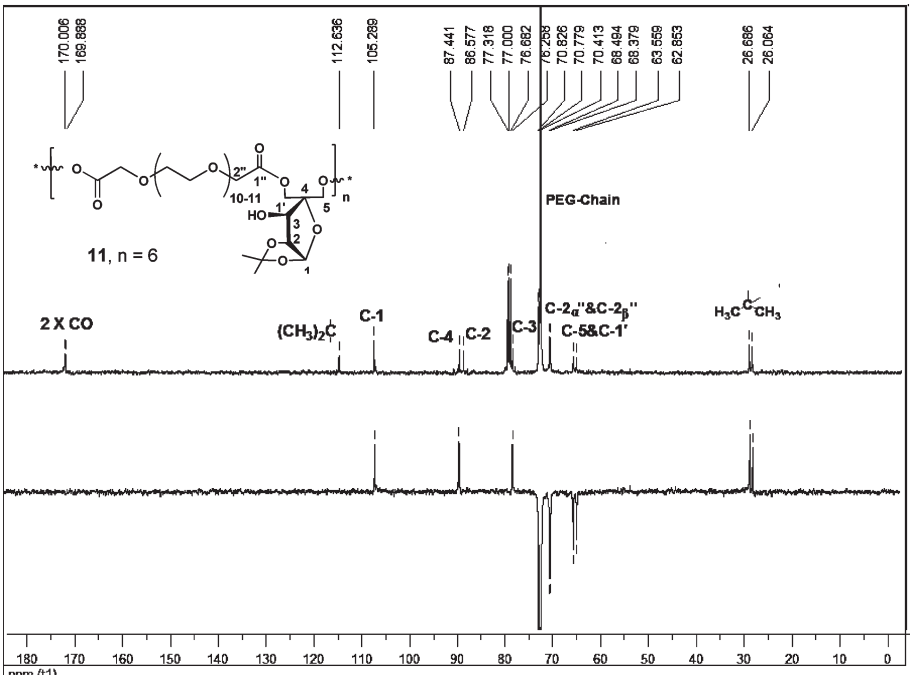

Figure 2. Comparison of ^{13}C and DEPT-135 NMR spectrum (Bruker DRX-400, 100 MHz, chloroform-*d*) of polymer **11**.

The presence of all other $-CH$, $-CH_2$, and $-CH_3$ groups in the polymer **12** was confirmed by its DEPT-135 NMR spectrum. The number-average molecular weight of the polymer **12** as obtained by GPC in THF (1 mL/min.) was 5682 g/mol with PDI of 1.11, which indicates the presence of approximately seven monomeric units in the polymer.

Poly[polyoxyethylene-oxy-bis(carboxymethyl)-4-methylene-1, 2-O-isopropylidene-3-O-pentyl-β-L-threo-pentofuranosyl] (***13***). In the ^{1}H NMR spectrum of polymer **13**, the C-5H and C-1″H recorded a downfield shift of 0.51 to 0.68 ppm and resonated at δ 4.09 to 4.39 (m) instead of δ 3.58 to 3.71 (m) with respect to the same protons in corresponding monomer 4-*C*-(hydroxymethyl)-1,2-*O*-isopropylidene-3-*O*-pentyl-β-L-*threo*-pentofuranose (**8**). The downfield shift in the chemical shift value of C-5H and C-1″H in the polymer revealed that the two primary hydroxyl groups at the corresponding positions in the starting compound **8** are engaged in transesterification

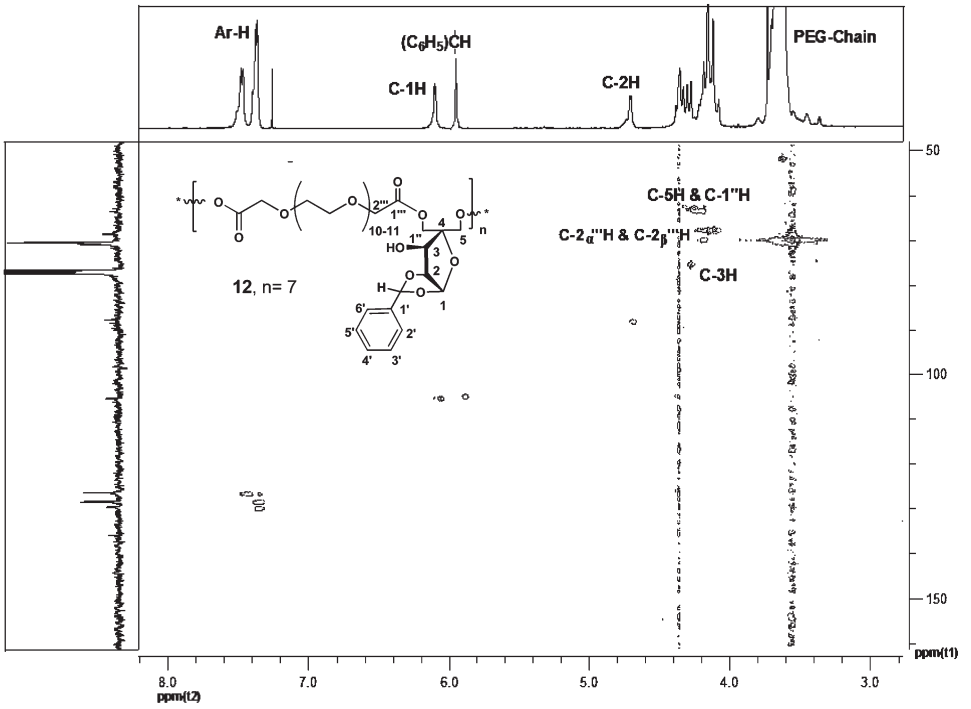

Figure 3. $^{1}H-^{13}C$ correlation spectrum (Bruker AMX-500, chloroform-*d*) of polymer **12**.

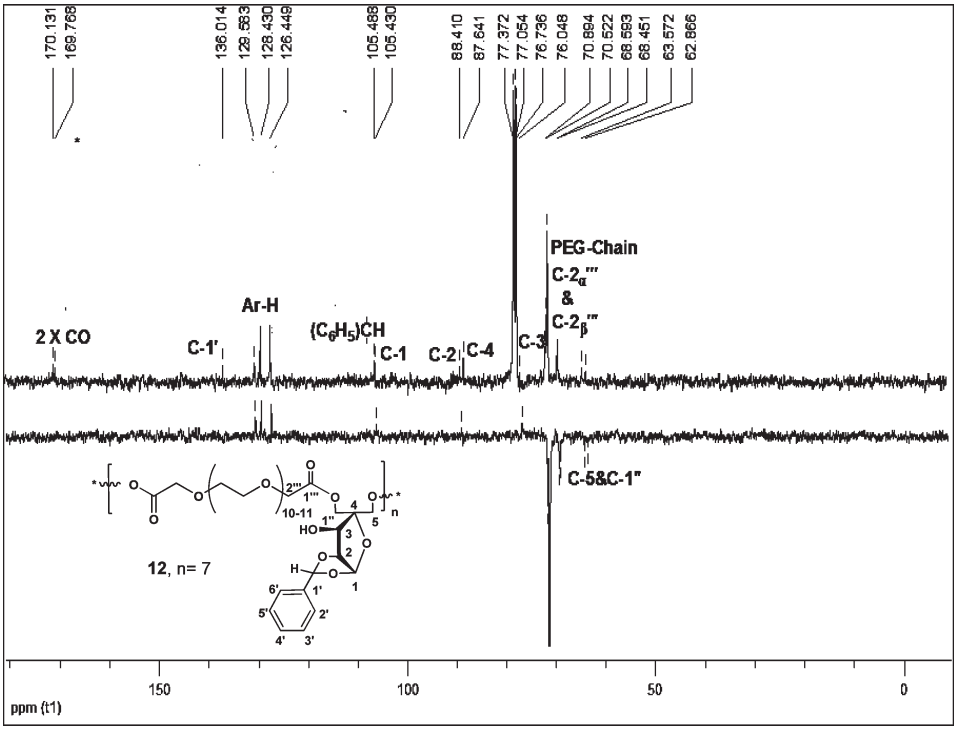

Figure 4. Comparison of ^{13}C and DEPT-135 NMR spectrum (Bruker DRX-400, 100 MHz, chloroform-*d*) of polymer **12**.

reaction with PEG dimethyl ester **10**. The presence of all other $-CH$, $-CH_2$, and $-CH_3$ groups in the polymer **13** was confirmed by its DEPT-135 NMR spectrum (Figure 5). The number-average molecular weight of the polymer **13** as obtained by GPC in THF (1 mL/min.) was 5882 g/mol with PDI of 1.26, which indicates the presence of approximately seven monomeric units in the polymer.

Aggregation Behavior in Aqueous Solution. To understand the aggregation behavior of the synthesized polymers **11**−**13** in aqueous solution, we investigated structural aspects of polymers using surface tension measurement and dynamic light scattering. Surface tension data were plotted as a logarithmic function of the surfactant concentration, where a break in the

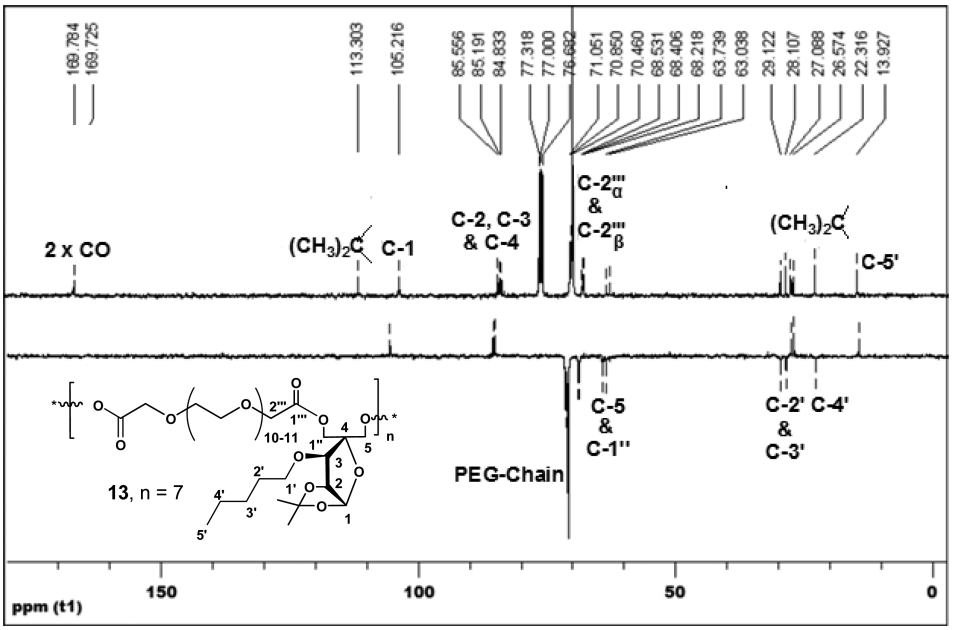

Figure 5. Comparison of ^{13}C and DEPT-135 NMR spectrum (Bruker DRX-400, 100 MHz, chloroform-*d*) of polymer **13**.

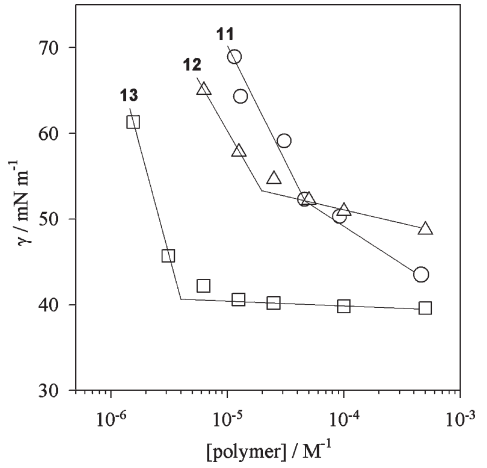

Figure 6. Surface tension (γ) versus log concentration of the sugar-PEG-based polymers **11** (○), **12** (Δ), and **13** (□) in aqueous solution at 25 °C. Measurements were performed in duplicate, and the surface tension obtained varied in the range of ±1 mN/m.

curve occurs at the CAC. As can be seen from the surface tension curves in Figure 6, polymers **11**−**13** were effective in reducing the surface tension (γ) of aqueous solution, thus showing a considerable decrease in γ as the polymer concentrations increased, followed by clear break point at CAC of the respective polymers. The CAC values obtained are equal to 4.5×10^{-5}, 2.0×10^{-5}, and 4.0×10^{-6} M for polymers **11**−**13**, respectively. From Figure 6, it is clearly observed that the attachment of a pentyl chain to the pentofuranose moiety promotes aggregation to a greater extent than a phenyl group. Thus, the CAC of copolymer **12** is approximately five times higher than that of copolymer **13**. The observed CAC of polymer **11** was found to be 2.2 fold higher than that of polymer **12** bearing benzylidene moiety. This shows that the absence of any hydrophobic moiety leads to the aggregation to a lesser extent.

Table 1. Critical Aggregation Concentration (CAC), Particle Size, and Polydispersity Index (PDI) of Micelles/Aggregates 11-13 in Aqueous Solution Measured by Light Scattering Method at 25°C

copolymer	CAC (M)	*z*-average diameter (nm)	PDI
11	4.5×10^{-5}	13[a]	0.241
12	2.0×10^{-5}	124[b]	0.207
13	4.0×10^{-6}	223[b]	0.105

[a] [**11**] = 5 g/L. [b] [**12**] and [**13**] = 1 g/L of polymers.

The precise size of the aggregates of polymers **11** to **13** in aqueous solution was determined by using dynamic light scattering. All polymers **11**−**13** were soluble in water as all sample solutions appeared clear. Measurements were carried out well above the CACs, that is, at a fixed polymer concentration of 1 g/L for polymers **12** and **13** and 5 g/L for polymer **11**. The results have been summarized in Table 1, and the corresponding size distribution profiles are displayed in Figure 7. For polymers **11**−**13** the hydrodynamic diameters were determined to be 13, 124, and 223 nm, respectively. A comparison of the intensity distribution profile with the corresponding volume and number distribution shows that all three compositions have a monomodal particle size distribution (Figure 7).

The aggregates of small size, d_H = 13 nm, can be regarded as polymeric micelles presumably with the pentofuranose building block making the core and the polyoxyethylene chain constituting the corona of the micelle (Figure 8).

There is a significant increase in the measured size as the pentofuranose moiety is modified with a phenyl group (polymer **12**) or a pentyl chain (polymer **13**). The order of magnitude obtained for **12** and **13** in aqueous solution does not correspond to simple polymeric micelles but rather to larger aggregates (clusters). Depending on the polymer concentration in water, the micelles may self-assemble to a loose network of aggregates formed because of intermicellar interactions through polyoxyethylene corona. Individual

micelles and clusters are in equilibrium; that is, the supramolecular network breaks and forms reversibly[37,38] (Figure 9). We assume that the aggregates of **12** and **13** are formed through an attractive interaction between the PEG moieties that constitute the corona of the micelles. The hydrophobic sugar moieties of the copolymers form the core of the micelles and are unlikely to contribute to intermicellar binding interactions. Furthermore, the copolymers **12** and **13** are not end-capped with hydrophobic moieties (hexadecyl, dodecyl, etc.), as discussed in the literature,[39−44] where aggregates are formed by hydrophobic interactions. Furthermore, such reports are there in the literature where intermicellar aggregates are formed through hydrophilic interaction of the polyethylene oxide chain in a dendritic structure. Therefore, dendritic multishell architectures bearing terminal monomethyl poly(ethylene glycol) (mPEG) outer shells were found to self-assemble into supramolecular aggregates in water.[45] Similar to the micelles/aggregates described herein, the terminal mPEG layer acts as an external polar layer, thus providing good solubility in aqueous solution. As shown by surface tension measurements and fluorescence spectroscopy, self-assembly spontaneously occurs above a well-defined threshold concentration (CAC).

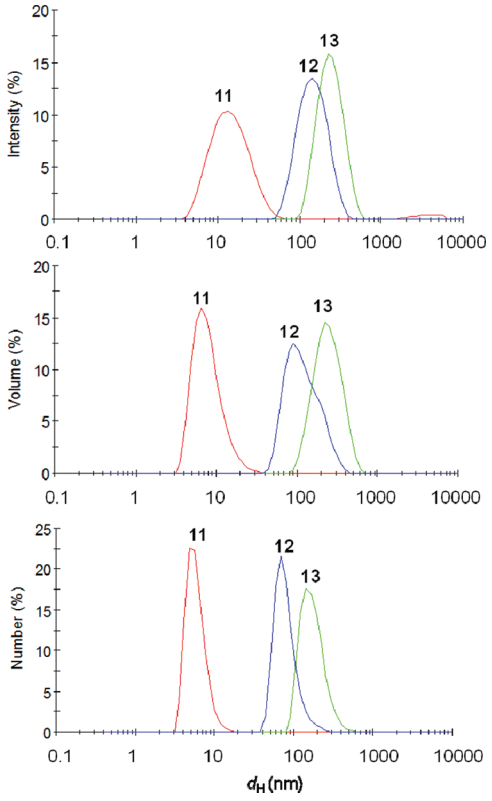

Figure 7. Size distribution profiles for aggregates of **11**−**13** in aqueous solution. The concentration of the polymers was fixed at 1 (polymers **12** & **13**) and 5 g/L (polymer **11**).

In conclusion, surface tension measurements and light scattering analysis have shown that modification of the pentofuranose unit has significant effects on CAC (aggregation behavior), the micelle/micellar aggregate formation, and their size distribution.

Structural analysis of the micelles and micellar assemblies of polymers **11**−**13** have also been investigated by means of transmission electron microscopy. As can be seen from Figure 10, all polymers showed nanoscopic spherical morphologies in aqueous media. For comparison purpose, aqueous sample solutions had the same concentration as that used in the case of DLS measurement, that is, 5 g/L for polymer **11** and 1 g/L for polymers **12** and **13**, respectively. The hydrodynamic diameters of micellar aggregates of hydrophobically modified polymers **12** and **13** are considerably higher than those estimated by TEM (Figure 10). This may be attributed to the high swelling capacity of micellar aggregates of polymers **12** and **13** in water. It is worth mentioning that the TEM analysis was carried out on dried samples, whereas light scattering experiments were performed on aqueous solutions. In fact, this behavior has been previously described by Aktas et al.,[46] who investigated the size distribution of chitosan and PEGylated chitosan nanoparticles (NPs) in aqueous solutions by means of dynamic light scattering and transmission electron microscopy.

Study of Encapsulation of Nile Red by Micelles/Aggregates of Polymer 11−13. The encapsulation properties of

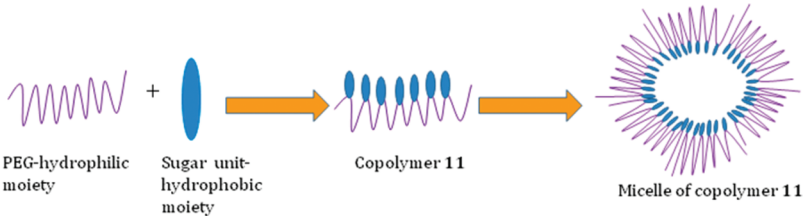

Figure 8. Proposed schematic representation of polymeric micelle copolymer **11** in aqueous solution.

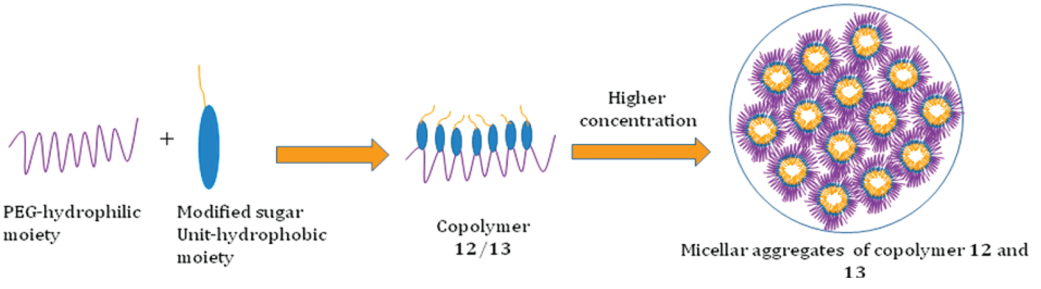

Figure 9. Proposed schematic representation of polymeric micellar aggregates of copolymer **12** and **13** in aqueous solution.

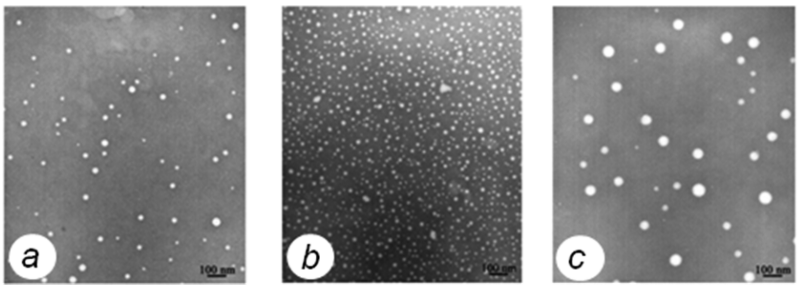

Figure 10. Transmission electron microscopy images of micelles of polymer **11** (a) and micellar aggregates of polymer **12** (b) and **13** (c). Spherical shape morphologies were observed with diameter in the range of 15−30 nm in the case of polymer **11** and 20−40 nm in the case of polymer **12**. Highly polydispersed spheres with diameter up to 60 nm were observed in case of polymer **13**. The scale bar is equal to 100 nm in all of the cases.

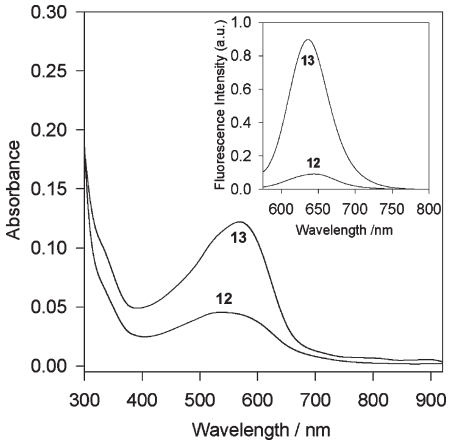

Figure 11. UV absorption of nile red solubilized by polymeric micelles of **12** and **13** in buffered aqueous solution (pH 7.4, 10 mM). Inset: corresponding fluorescence emission spectra of nile red (λ_{exc} = 550 nm) in the presence of **12** and **13**, respectively.

copolymers **11**−**13** were spectroscopically investigated by using the water-insoluble hydrophobic model dye nile red. In recent years, nile red has been extensively used as a probe for solvent polarity and hydrophobicity.[47] Nile red is particularly beneficial in sensing the micropolarity of modified polymers in aqueous solution.

For the encapsulation experiments, a 10 mM nile red stock solution was freshly prepared by dissolving an appropriate amount of the dye in dry THF. Aliquots (25 μL) were added to 1.0 mL of the aqueous polymer solutions (1.0 mg/mL) in phosphate buffer (100 mM) of pH 7.4, and after subsequent removal of the organic solvent, the obtained aqueous solutions were stirred for at least 18 h at room temperature. The mixture was filtered through a syringe filter (Rotilabo, 0.45 μm pore size) to remove the insoluble excess of nile red. The colored aqueous solutions of the polymers **12** and **13** were then analyzed by means of UV/vis and fluorescence spectroscopy.

As can be seen from Figure 11, the λ_{max} values for the UV/vis spectra of nile-red-loaded buffered aqueous solution of polymer **12** and **13** are 530 and 568 nm, respectively. These data clearly suggest a considerable change in the microenvironment for solubilized dye. Nile red is a solvatochromic dye molecule and can be used to probe the polarity or rather the effective dielectric constant of its (micro)environment. The solvatochromic behavior of nile red is such that the absorption and emission maxima strongly depend on the polarity of the environment (solvent). We have chosen ethylene glycol and PEG 400 as model systems "to probe the microenvironment" of encapsulated nile red molecules. The maximum of the absorption band is hypsochromically shifted from 557 to 540 nm on going from ethyleneglycol (ε = 37.7) to PEG 400 (ε = 14.3) as solvent. Hence, from the spectroscopic results, it can be inferred that the solubilization of nile red appears to primarily take place, at least to an appreciable extent, within the poly(oxyethylene) layer of **12** and **13**. All copolymers are noncharged and consist of a polyoxyethylene backbone to which functionalized pentofuranose-based moieties are attached. In this context, it is important to note that apart from the PEG chains only water molecules and ions (buffer) contribute to the polarity of the hydrophilic poly(oxyethlene) region. This might lead to differences in the observed wavelength of the absorption maxima when comparing with neat ethyleneglycol and PEG 400, respectively.

The inset in Figure 11 shows the corresponding fluorescence emission spectra. Both the buffered aqueous solutions of nile-red-loaded polymeric aggregates of polymers **12** and **13** were given excitation at 550 nm. Excitation of the dye present in the buffered aqueous solution of polymeric aggregates of **12** results in a relatively low fluorescence with a λ_{max} of 645 nm. On the contrary, in the presence of **13**, the fluorescence intensity is roughly nine times higher than that for **12**. At the same time, the maximum of the emission band is slightly shifted to a lower wavelength of 635 nm. The spectroscopic results therefore imply that in the presence of polymeric aggregates of polymer **13**, the solubilized dye essentially experiences a more hydrophobic environment.

At first sight, it appears paradoxical that we found a maximum absorbance at 530 and 568 nm for **12** and **13**, respectively. To our surprise, however, we have observed that with increasing amount of nile red stock solution, the absorption band undergoes a hypsochromic shift to a much shorter wavelength with a maximum in the 450−500 nm range, accompanied by an intense shoulder in the red region of the spectrum. This unusual spectroscopic behavior suggests strong binding interactions between the dye molecules. The self-association of dyes in solution is a well-known phenomenon in dye chemistry owing to noncovalent (supramolecular) binding interactions between the molecules. Therefore, we have chosen a quite low amount (25 μL) of nile red stock solution. In this regard, it is worth mentioning a recent report by Varghese and Wagenknecht,[48] who investigated the noncovalent self-assembly of nile-red-modified 2-deoxyuridine in water. They found that the absorption spectrum in water (ε = 78) shows a maximum at 540 nm, which is 30 nm blueshifted relative to the maximum in methanol (570 nm, ε = 32). This unusual hypsochromic shift has been assigned to the formation of H-type

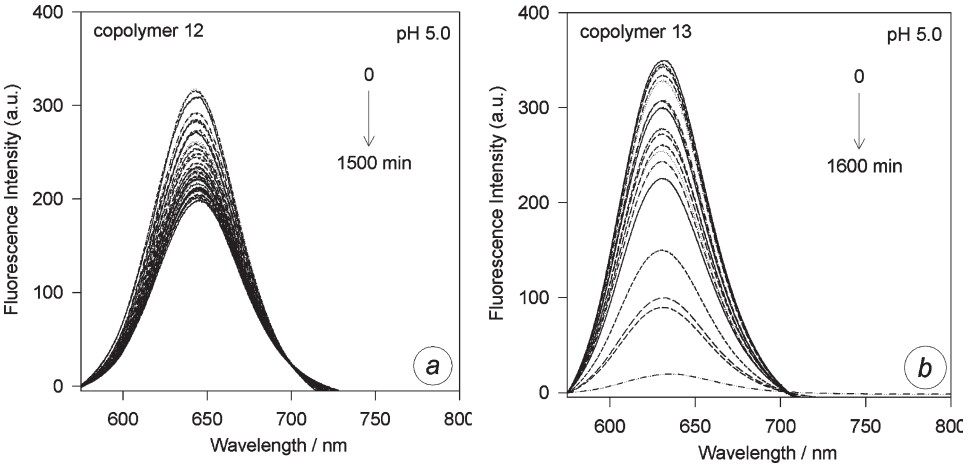

Figure 12. Fluorescence intensity curves observed at different time intervals during release of nile red from aggregates of copolymer s**12** and **13** in buffered aqueous solution of pH 5 at 37 °C. Change in fluorescent intensity (a.u.) versus wavelength (nm) for copolymers **12** (a) and **13** (b). Observed fluorescence intensity (a.u.) decreases with time in acidic pH 5.0.

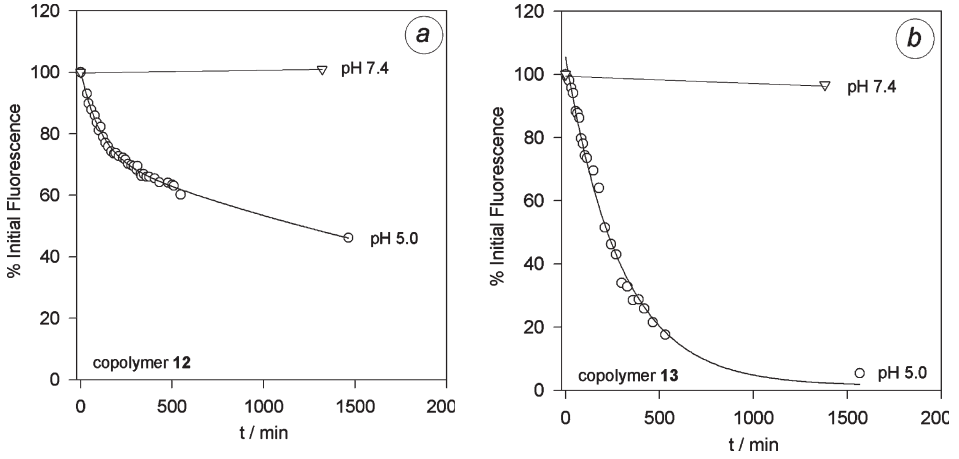

Figure 13. Release of nile red from aggregates of copolymers **12** and **13** in buffered aqueous solutions of pH 5.0 and physiological pH 7.4 at 37 °C. Percentage initial maximum fluorescence observed at different time intervals for copolymers **12** (a) and **13** (b).

aggregates in water. We therefore assume that in the presence of **12**, nile red tends to form dye−polymer(dye) aggregates in buffer, in accord with an absorption maximum at 530 nm. For polymer **13**, however, a considerable higher amount of dye is required. Under the experimental condition employed, self-assembly is less favored, and solubilized dye molecules exist to an appreciable extent as monomers, thus showing an absorption maximum at 568 nm. At the present, we cannot offer direct evidence of the assumption. This phenomenon, however, is currently under investigation.

Finally, no noticeable absorbance was detected upon the addition of **11**. This indicates that the hydrophobic dye molecules reside preferably at the aqueous bulk phase.

Release of Nile Red. Our particular interest in the present study was to investigate the polymeric micellar aggregates of **12** and **13** as controlled drug release vehicles. Therefore, we studied the time-dependent release of solubilized nile red at acidic pH (5.0, 37 °C) by using fluorescence spectroscopy.[49−51]

We followed the protocol previously described by Gillies et al.[51] in which the polymers were first equilibrated with nile red overnight in 10 mM phosphate buffer (pH 7.4). The solution was divided into two samples; the pH of the one sample was adjusted to pH 5.0 by the addition of a small aliquot of concentrated acetate buffer (4 M). The second sample was maintained at pH 7.4, but the salt concentration was adjusted to the same as that above by the addition of the concentrated phosphate buffer (2 M). To exclude any effect due to changes of salt concentration, the two samples were adjusted to the same salt concentration of 100 mM.

In acidic solution of pH 5.0, the polymeric micellar aggregates of **12** and **13** exhibited a significant decrease in the maximum intensity with time, whereas the same nile-red-loaded systems were not affected at physiological pH 7.4 (Figures 12 and 13). This suggests that our polymeric systems respond to subtle pH changes in the physiological environment. The plot of % initial fluorescence versus time obtained was used to estimate the half-life time of dye release. Data were fitted to the relation $I_t = I_0 \cdot \exp(-k_{obs} \cdot t)$, and the half-life time was found to be 3.4 and 2.0 h ($r^2 \geq 0.990$) for **12** and **13**, respectively. For polymeric aggregates of **13**, a complete release was observed in ~25 h. On the contrary, the % initial fluorescence was reduced to only half of its intensity when polymer **12** was used. The in vitro release

profiles of the solubilized dye determined at acidic pH have shown that the two copolymers have good potential for the controlled release of hydrophobic drug molecules.

CONCLUSIONS

A new biocatalytic route has been designed and developed to synthesize three novel sugar-PEG-based amphiphilic polymers **11**−**13** by copolymerization of functionalized pentofuranose backbone with PEG-600 dimethyl ester using Novozyme-435. Regioselectivity has been exhibited in the polymerization of monomers **2** and **5** with PEG dimethyl ester, where PEGylation occurs only at the primary hydroxyl groups leading to the formation of polymers **11** and **12**. All three polymers have been explored for drug delivery application. Attachment of phenyl and pentyl moieties to the pentofuranose backbone in the copolymers **12** and **13**, respectively, leads to the formation of supramolecular aggregates of diameters 124 and 223 nm, respectively, in the aqueous solution, as observed by DLS. Supramolecular aggregates of polymers **12** and **13** were capable to encapsulate nile red molecule, as revealed by the guest enacapsulation studies done in buffered aqueous solutions. Nile red release in case of polymer **13** was found to be faster with a half-life time of 2.0 h than that in the polymer **12** with a half-life time of 3.4 h at acidic pH 5.0 (37 °C). No release was observed at physiological pH 7.4 (37 °C), as observed by fluorescence studies of nile-red-loaded aggregates. Further studies are in progress to achieve the lead polymeric architectures with higher drug loading capacity and longer lasting release profiles.

ASSOCIATED CONTENT

Supporting Information. Experimental details of synthesis of monomers and copolymers, ^{1}H NMR and ^{13}C NMR spectra of compounds **2**−**8** and for copolymers **11**−**13**, DEPT-135 NMR spectra of compounds **4**−**8** and for copolymers **11**−**13**, $^{1}H-^{1}H$ COSY spectrum of copolymer **13**, and gel permeation chromatograms of copolymers **11**−**13**. This material is available free of charge via the Internet at http://pubs.acs.org.

AUTHOR INFORMATION

Corresponding Author

*(R.H.) Tel: +49-30-838-52633; Fax: +49-30-838-53357; E-mail: haag@chemie.fu-berlin.de. (A.K.P.) Tel: 00-91-11-27662486; E-mail: ashokenzyme@yahoo.com.

ACKNOWLEDGMENT

We thank the Department of Biotechnology (DBT, New Delhi, India) and the International Bureau (IB) of the Federal Ministry of Education and Research (BMBF, Bonn, Germany) and the University of Delhi under the DU-DST Purse grant for financial assistance to this work. S.B. thanks Institute for Chemistry and Biochemistry, Free University Berlin, Germany for providing the opportunity and infrastructure to accomplish a part of this work. S.B. and D.M. thank UGC, New Delhi for the award of research fellowship.

REFERENCES

(1) Francesco, M. V.; Gianfranco, P. *Drug Discovery Today* **2005**, *10*, 1451–1458.
(2) Nakamura, T.; Nagasaki, Y.; Kataoka, K. *Bioconjugate Chem.* **1998**, *9*, 300–303.
(3) Koyama, Y.; Ishikawa, M.; Iwamoto, M.; Kojima, S. *J. Controlled Release* **1992**, *22*, 253–261.
(4) Cammas, S.; Suzuki, K.; Sone, C.; Sakurai, Y.; Kataoka, K.; Okano, T. *J. Controlled Release* **1997**, *48*, 157–164.
(5) Chung, J. E.; Yokoyama, M.; Okano, T. *J. Controlled Release* **2000**, *65*, 93–103.
(6) Engin, K.; Leeper, D. B.; Cater, J. R.; Thistlethwaite, A. J.; Tupchong, L.; McFarlane, J. D. *Int. J. Hypertherm.* **1995**, *11*, 211–216.
(7) van Sluis, R.; Bhujwalla, Z. M.; Ballerteros, P.; Alverez, J.; Cerdan, S.; Galons, J. P.; Gillies, R. J. *Magn. Reson. Med.* **1999**, *41*, 743–750.
(8) Ojugo, A. S. E.; Mesheehy, P M. J.; McIntyre, D. J. O.; McCoy, C.; Stubbs, M.; Leach, M. O.; Judson, I. R.; Griffiths, J. R. *NMR Biomed.* **1999**, *12*, 495–504.
(9) Calderon, M.; Quadir, M. A; Strumia, M.; Haag, R. *Biochimie* **2010**, *92*, 1242–1251.
(10) Gillies, E. R.; Frechet, J. M. J. *Bioconjugate Chem.* **2005**, *16*, 361–368.
(11) Haag, R. *Angew. Chem., Int. Ed.* **2004**, *43*, 278–282.
(12) Haag, R.; Kratz, F. *Angew. Chem., Int. Ed.* **2006**, *45*, 1198–1215.
(13) Gillies, E. R.; Frechet, J. M. J. *Pure Appl. Chem.* **2004**, *76*, 1295–1307.
(14) Yoo, H. S.; Lee, E. A.; Park, T. G. *J. Controlled Release* **2002**, *82*, 17–27.
(15) Satturwar, P.; Eddine, M. N.; Ravenelle, F.; Leroux, J.-C. *Eur. J. Pharm. Biopharm.* **2007**, *65*, 379–387.
(16) Jang, W.-D.; Nishiyama, N.; Zhang, G.-D.; Harada, A.; Jiang, D.-L.; Kawauchi, S.; Morimoto, Y.; Kikuchi, M.; Koyama, H.; Aida, T.; Kataoka, K. *Angew. Chem., Int. Ed.* **2005**, *44*, 419–423.
(17) Chen, W.; Meng, F.; Li, F.; Ji, S.-J.; Zhong, Z. *Biomacromolecules* **2009**, *10*, 1727–1735.
(18) Chen, W.; Meng, F.; Cheng, R.; Zhong, Z. *J. Controlled Release* **2010**, *142*, 40–46.
(19) Youssefyeh, R. D.; Verheyden, J. P. H.; Moffatt, J. G. *J. Org. Chem.* **1979**, *44*, 1301–1309.
(20) Christensen, S. M.; Hansen, H. F.; Koch, T. *Org. Process Res. Dev.* **2004**, *8*, 777–780.
(21) Yang, K. L.; Blackman, B.; Diederich, W.; Flaherty, P. T.; Mossman, C. J.; Roy, S.; Ahn, Y. M.; Georg, G. I. *J. Org. Chem.* **2003**, *68*, 10030–10039.
(22) Crich, D.; Li, M. *J. Org. Chem.* **2008**, *73*, 7003–7010.
(23) Yu, S.-H.; Wang, H.-Y.; Chiang, L.-W.; Pei, K. *Synthesis* **2007**, *9*, 1412–1420.
(24) Prasad, A. K.; Kalra, N.; Yadav, Y.; Kumar, R.; Sharma, S. K.; Patkar, S.; Lange, L.; Wengel, J.; Parmar, V. S. *Chem. Commun.* **2007**, 2616–2617.
(25) Dueno, E. E.; Chu, F.; Kim, S.-I.; Jung, K. W. *Tetrahedron Lett.* **1999**, *40*, 1843–1846.
(26) Dhavale, D. D.; Matin, M. M. *Tetrahedron* **2004**, *60*, 4275–4281.
(27) Gupta, S.; Pandey, M. K.; Levon, K.; Haag, R.; Watterson, A. C.; Parmar, V. S.; Sharma, S. K. *Macromol. Chem. Phys.* **2010**, *211*, 239–244.
(28) Faber, K. *Biotransformations in Organic Chemistry*, 5th ed.; Springer-Verlag: Berlin, 2004.
(29) Drauz, K.; Waldmann, H. *Enzyme Catalysis in Organic Synthesis*; VCH: Weinheim, Germany, 1994; Vols. 1 and 2.
(30) Prasad, A. K.; Kalra, N.; Yadav, Y.; Singh, S. K.; Sharma, S. K.; Patkar, S.; Lange, L.; Olsen, C. E.; Wengel, J.; Parmar, V. S. *Org. Biomol. Chem.* **2007**, *5*, 3524–3530.
(31) Maity, J.; Shakya, G.; Singh, S. K.; Ravikumar, V. T.; Parmar, V. S.; Prasad, A. K. *J. Org. Chem.* **2008**, *78*, 5629–5632.
(32) Singh, S. K.; Sharma, V. K.; Olsen, C. E.; Wengal, J.; Parmar, V. S.; Prasad, A. K. *J. Org. Chem.* **2010**, *75*, 7932–7935.
(33) Kumar, R.; Chen, M.-H.; Parmar, V. S.; Samuelson, L. A.; Kumar, J.; Nicolosi, R.; Yoganathan, S.; Watterson, A. C. *J. Am. Chem. Soc.* **2004**, *126*, 10640–10644.

(34) Kumar, R.; Shakil, N. A.; Chen, M.-H.; Parmar, V. S.; Samuelson, L. A.; Kumar, J.; Watterson, A. C. *J. Macromol. Sci., Part A: Pure Appl.Chem.* **2002**, *A39*, 1137–1149.
(35) Sharma, S. K.; Husain, M.; Kumar, R.; Samuelson, L. A.; Kumar, J.; Watterson, A. C.; Parmar, V. S. *Pure Appl. Chem.* **2005**, *77*, 209–226.
(36) Malhotra, S.; Calderon, M.; Prasad, A. K.; Parmar, V. S.; Haag, R. *Org. Biomol. Chem.* **2010**, *8*, 2228–2237.
(37) Hussain, H.; Busse, K.; Kressler, J. *Macromol. Chem. Phys.* **2003**, *204*, 936–946.
(38) Yang, J.; Zhang, D.; Jiang, S.; Yang, J.; Nie, J. *J. Colloid Interface Sci.* **2010**, *352*, 405–414.
(39) Berret, J.-F.; Calvet, D.; Collet, A.; Viguier, M. *Curr. Opin. Colloid Interface Sci.* **2003**, *8*, 296–306.
(40) Alami, E.; Almgren, M.; Brown, W.; François, J. *Macromolecules* **1996**, *29*, 2229–2243.
(41) Chassenieux, C.; Nicolai, T.; Durand, D. *Macromolecules* **1997**, *30*, 4952–4958.
(42) Xu, B.; Yetka, A.; Li, L.; Masoumi, Z.; Winnik, M. A. *Colloids Surf., A* **1996**, *112*, 239–250.
(43) Xu, B.; Yetka, A.; Winnik, M. A.; Sadeghy-Dalivand, K.; James, D. F.; Jenkins, R.; Basset, D. *Langmuir* **1997**, *13*, 6903–6911.
(44) Le Meins, J.-F.; Tassin, J.-F. *Colloid Polym. Sci.* **2003**, *281*, 283–287.
(45) Radowski, M. R.; Shukla, A.; Berlepsch, H. V.; Bottcher, C.; Pickaert, G.; Rehage, H.; Haag, R. *Angew. Chem., Int. Ed.* **2007**, *46*, 1265–1269.
(46) Aktas, Y.; Yemisci, M.; Andrieux, K.; Gursoy, R. N.; Alonso, M. J.; Fernandez-Megia, E.; Novoa-Carballal, R.; Quinoa, E.; Riguera, R.; Sargon, M. F.; Celik, H.; Demir, A. S.; Hıncal, A. A.; Dalkara, T.; Capan, Y.; Couvreur, P. *Bioconjugate Chem.* **2005**, *16*, 1503–1511.
(47) Jee, A.-Y.; Park, S.; Kwon, H.; Lee, M. *Chem. Phy. Lett.* **2009**, *477*, 112–115.
(48) Varghese, R.; Wagenknecht, H.-A. *Chem. Eur. J.* **2010**, *16*, 9040–9046.
(49) Greenspan, P.; Mayer, E. P.; Fowler, S. D. *J. Cell Biol.* **1985**, *100*, 965–973.
(50) Krishna, M. M. G. *J. Phys. Chem. A* **1999**, *103*, 3589–3595.
(51) Gillies, E. R.; Jonsson, T. B.; Frechet, J. M. J. *J. Am. Chem. Soc.* **2004**, *126*, 11936–11943.